SYNTHESIS AND CHARACTERIZATION OF NANOCRYSTALLINE CdS THIN FILMS BY MICROWAVE-ASSISTED CHEMICAL BATH DEPOSITION FOR PHOTODETECTORS APPLICATION

MOHAMMED HUSHAM MOHAMMED ALI

UNIVERSITI SAINS MALAYSIA

2015

SYNTHESIS AND CHARACTERIZATION OF NANOCRYSTALLINE CdS THIN FILMS BY MICROWAVE-ASSISTED CHEMICAL BATH DEPOSITION FOR PHOTODETECTORS APPLICATION

by

MOHAMMED HUSHAM MOHAMMED ALI

Thesis submitted in fulfillment of requirements for the degree of Doctor of Philosophy

October 2015

ACKNOWLEDGEMENTS

First and foremost, I would like to thank Allah for granting me health and patience to complete this research. I would like to express my sincere gratitude to my main supervisor, Prof. Dr. Zainuriah Hassan, for her scholarly guidance and dedicated time and support throughout the course of this study. Thanks again Prof. for having your door open every time I needed help, even though you never had the time, you always made it.

Much of this work would have been virtually impossible without the technical support offered by our helpful laboratory assistants at the School of Physics, Universiti Sains Malaysia.

Last, and most important, I extend special thanks to my family for supporting me during this important time. Without their endless love, patience and support, I could not have a chance to complete this study. I thank all my friends and colleagues who supported me and helped me at the School of Physics in Universiti Sains Malaysia.

M. Husham

15th Oct 2015

Penang-Malaysia

TABLE OF CONTENTS

		Page
ACKNOWLEDGEMENTS		**ii**
TABLE OF CONTENTS		**iii**
LIST OF TABLES		**vii**
LIST OF FIGURES		**viii**
LIST OF ABBREVIATIONS		**xii**
LIST OF SYMBOLS		**xiii**
ABSTRAK		**xv**
ABSTRACT		**xviii**
CHAPTER1: INTRODUCTION		1
1.1	Introduction	1
1.2	Problem statement	2
1.3	Scope of study	3
1.4	Objectives of this study	4
1.5	Originality of this research	4
1.6	Outline of the thesis	5
CHAPTER 2: LITERATURE REVIEW		6
2.1	Introduction	6
	2.2.1 CdS	6
	2.2.2 Nanocrystalline CdS thin films prepared by CBD	7

2.2.3 Nanostructured CdS prepared by MA-CBD 11

2.2.4 Nanostructured CdS-based PDs 14

CHAPTER 3: THEORETICAL BACKGROUND 18

3.1 Introduction 18

3.2 CBD technique 18

3.2.1 Mechanisms of the CBD technique 20

3.2.1 MA-CBD 23

3.3 Structural properties of CdS 26

3.4 Optical properties of CdS 28

3.5 Metal–semiconductor contacts theory 29

3.5.1 Ohmic contacts 30

3.5.2 Schottky contacts 31

3.6 Theoretical concept of PDs 34

3.7 MSM PDs 36

3.7.1 Operational parameters of PDs 37

3.7.1.1 Responsivity (*R*) 37

3.7.1.2 Sensitivity (*S*) 38

3.7.1.3 Quantum efficiency (QE) 38

3.7.1.4 Response and recovery times 38

CHAPTER 4: METHODOLOGY AND CHARACTERIZATION TOOLS 40

4.2.1 Growth of nanocrystalline CdS thin films on Si(100) substrates using different molar concentrations of precursors 40

4.2.2 Growth of nanocrystalline CdS thin films on Si(100) substrates at different deposition times 43

4.2.3 Growth of nanocrystalline CdS thin films on Si(100) with different S/Cd molar ratios 43

4.3 PD device fabrication 43

4.3.1 Metal contacts deposition 44

4.4 Characterization tools and working principle 45

4.4.1 XRD 46

4.4.2 FESEM with EDX 48

4.4.3 AFM 50

4.4.4 Thin-film thickness measurements 52

4.4.5 PL spectroscopy 54

4.4.6 Photodetection measurements 56

4.5 Summary 57

CHAPTER 5: RESULTS AND DISCUSSION CHARACTERIZATION OF NANOCRYSTALLINE CdS THIN FILMS 58

5.1 Introduction 58

5.2 Growth of nanocrystalline CdS thin films using different molar concentration of ions sources 58

5.2.1 FESEM and EDX characterization 58

5.2.2 AFM analysis 62

5.2.3 Structural analysis 62

5.2.4 PL measurements 67

5.3 Growth of nanocrystalline CdS thin films at different deposition times 69

5.3.1 FESEM and EDX Characterization 69

5.3.2 AFM measurements 72

5.3.3 Structural properties 72

5.3.4 PL measurements 75

5.4 Growth of nanocrystalline CdS thin films using different S/Cd molar ratios 78

5.4.1 FESEM and EDX characterization 78

5.4.2 AFM measurements 81

5.4.3 XRD analysis 81

5.4.4 PL measurements 84

5.5 Summary 87

CHAPTER 6: RESULTS AND DISCUSSION PHOTODETECTOR DEVICES 88

6.1 Introduction 88

6.2 Characterization of CdS thin film-based PD 88

6.3 MSM PDs based on nanocrystalline CdS thin films grown at different deposition times 93

6.4 MSM PDs based on nanocrystalline CdS thin films grown using different S/Cd molar ratios 99

6.4.1 Characterization of the self-powered PDs 105

6.5 Summary 108

CHAPTER 7: CONCLUSIONS AND FUTURE WORK 110

7.1 Conclusions 110

7.2 Future studies 112

REFERENCES 113

APPENDICES 127

9.1 Appendix A 127

9.2 Appendix B 128

PUBLICATIONS 129

LIST OF TABLES

Page

Table 2.1: Electrical, thermal, mechanichal and optical properties for CdS 7

Table 2.2: Photoresponse properties of CdS-based PDs fabricated using different fabrication methods. 17

Table 3.1: The electrical nature of ideal metal–semiconductor contacts. 30

Table 5.1: EDX analysis of nanocrystalline CdS thin films prepared using different molar concentrations of precursors. 61

Table 5.2: Summery of XRD analysis for the grown CdS thin films using different molar concentration of precursors. 66

Table 5.3: Summary of XRD analysis for CdS thin films prepared at different deposition times. 75

Table 5.4: PL spectra summary for CdS thin films prepared using different deposition times. 77

Table 5.5: Thickness and S/Cd content for CdS thin films prepared using different S/Cd molar ratios. 79

Table 5.6: XRD analysis summary for nanaocrystalline CdS thin films grown using different S/Cd molar ratios. 84

Table 5.7: PL spectra summary for CdS thin films prepared using different S/Cd molar ratios. 87

Table 6.1: Photoresponse properties of the fabricated PD under illumination to 500 nm light wavelength. 92

Table 6.2: Summary of electrical and photoresponse properties for fabricated PDs based on nanocrystalline CdS thin films prepared at deposition times of 10, 20, and 30 min. 98

Table 6.3: Summary of electrical and photoresponse properties for fabricated PDs A*, B* and C. 105

Table 6.4: Photoresponse properties for the fabricated PDs A* and B* in comparison with other reported CdS-based PDs. 108

LIST OF FIGURES

Page

Figure 3.1: Schematic of CBD-CdS thin film via (a, b, and c) ion-by-ion mechanism and (d, e, and f) cluster mechanism. Adopted from. 23

Figure 3.2: Uniform distribution of heat inside the reaction vessel using microwave compared with temperature gradients occurred by the conventional heating method. 24

Figure 3.3: Hexagonal and cubic structures of CdS. Adopted from. 27

Figure 3.4: Energy band diagram of a metal and n-type semiconductor (a) before and (b) after contact for $\Phi M < \Phi S$. 31

Figure 3.5: Energy band diagram of a metal and n-type semiconductor (a) before and (b) after contact for $\Phi M > \Phi S$. 32

Figure 3.6: Plot of ln I as a function of V. 33

Figure 3.7: Schematic of carriers photo-excitation. 35

Figure 3.8: Diagram illustrates the photodetection process. 35

Figure 3.9: Basic structure of an MSM PD: (a) top view, (b) cross-sectional view. 37

Figure 3.10: Response and recovery times of a typical PD which was exposed to pulse light source. 39

Figure 4.1: Preparation steps of nanocrystalline CdS thin films on Si substrates using MA-CBD approach. 41

Figure 4.2: Flow chart of the preparation process for nanocrystalline CdS thin films on Si substrates, and photodetector devices fabrication. 42

Figure 4.3: Thermal evaporation system. 44

Figure 4.4: (a) Geometry of metalic electrodes (b) schematic illustration for the fabricated MSM PD. 45

Figure 4.5: Bragg diffraction from a cubic crystal lattice. The angles at which diffraction occurs are a function of the distance between planes and the X-ray wavelength. 47

Figure 4.6: HR-XRD system with a schematic diagram of an X-ray diffraction experiment. 48

Figure 4.7: Field emission scanning electron microscope (FESEM). 49

Figure 4.8: Schematic diagram of FESEM. 50

Figure 4.9: Dimension edge, Bruker AFM equipment. 52

Figure 4.10: Schematic diagram for atomic force microscopy. The sample exerts a force on the probe tip on top of a cantilever whose deflection is detected. 52

Figure 4.11: (a) Filmetrics F20 system (b) a schematic illustration for thin film thickness measurement. 53

Figure 4.12: PL instrument setup configuration. 55

Figure 4.13: Renishaw inVia PL spectroscopy system. 55

Figure 4.14: Schematic of experimental setup for photodetection measurements. Adopted and redrawn from. 56

Figure 5.1: FESEM images for CdS thin films grown on Si(100) by MACBD using different precursors concentration of (a) 0.04, (b) 0.06, (c) 0.08 and (d) 0.10 M. 60

Figure 5.2: EDX spectra of CdS thin films grown using different molar concentrations of precursors: (a) 0.04, (b) 0.06, (c) 0.08 M and (d) 0.10 M. 61

Figure 5.3: AFM images for nanocrystalline CdS thin films grown using different molar concentrations of precursors: (a) 0.04, (b) 0.06, (c) 0.08 and (d) 0.10 M. 63

Figure 5.4: Rrms as a function of ion sources molar concentration shows the surface roughness variation with precursor molar concentration. 64

Figure 5.5: XRD patterns of nanocrystalline CdS thin films grown on Si(100) substrates using different molar concentration of precursors. 65

Figure 5.6: Room-temperature PL spectra of nanocrystalline CdS thin films grown using different molar concentration of precursors. 68

Figure 5.7: PL peak intensity and NBE/DLE ratio of the prepared CdS thin films as a function of precursors molar concentration. 69

Figure 5.8: FESEM with EDX analysis for CdS thin films prepared at deposition times of: (a) 10, (b) 20, and (c) 30 min. 71

Figure 5.9: AFM images for CdS thin films grown at deposition times of (a) 10 (b) 20, and (c) 30 min. 73

Figure 5.10: XRD patterns for nanaocrystalline CdS thin films grown on Si(100) substrates via MA-CBD at different deposition times of (a) 10, (b) 20, and (c) 30 min. 74

Figure 5.11: Room-temperature PL spectra of nanocrystalline CdS thin films grown at different deposition times of (a) 10, (b) 20, and (c) 30 min. 77

Figure 5.12: FE-SEM images along with EDX analysis spectra for nanocrystalline CdS thin films grown using S/Cd molar ratios of (a) 1.25, (b) 1.875 and (c) 2.5. 80

Figure 5.13: AFM images for CdS thin films grown using different S/Cd molar ratio of (a) 1.25, (b) 1.875 and (c) 2.5. 82

Figure 5.14: XRD patterns for nanaocrystalline CdS thin films grown on Si(100) substrates using S/Cd molar ratios of (a) 1.25, (b) 1.875, and (c) 2.5. 83

Figure 5.15: Room-temperature PL spectra of nanocrystalline CdS thin films grown using different S/Cd molar ratios. 86

Figure 6.1: *I–V* measurement for the fabricated PD under dark and illumination to low power (1.20 mW/cm2) 500 nm light. 89

Figure 6.2: Spectral response shows the responsivity curve of the fabricated PD as a function of incident light wavelength, at a fixed applied bias of -1 V. 90

Figure 6.3: (a) Response time for the fabricated PD under illumination to 500 nm chopped light at applied biases of −0.5 and −1 V. (b) A magnified (on/off) photoresponse cycle for the fabricated PD. 91

Figure 6.4: *I–V* measurements for the fabricated PDs (a) device A and (b) device B under dark and illumination to low power (1.20 mW/cm2) 500 nm light. 94

Figure 6.5: Spectral response shows the responsivity curves of the fabricated PDs A and B as a function of incident light wavelength, at a fixed applied bias of -1 V. 95

Figure 6.6: (a) Response time for the fabricated PDs A and B under illumination to 500 nm chopped light at an applied bias of −1 V. (b) A magnified (on/off) photoresponse cycle for the fabricated PDs. 97

Figure 6.7*: I–V* characteristics for the fabricated PDs in the dark and under 500-nm light illumination (a) device A*, (b) device B* and (c) device C. The insets showed the rectification characteristic for the fabricated PDs. 101

Figure 6.8: Spectral response curves for the fabricated PDs A*, B* and C at a fixed applied bias of −1 V. 102

Figure 6.9: Response time for the fabricated PDs A*, B* and C with a magnified on/off cycle, measured under illumination to 500 nm chopped light at an applied bias of −1 V. 104

Figure 6.10: Spectral response curves for the fabricated PDs A* and B* at zero applied bias. 106

Figure 6.11: (a) Response time for the fabricated PDs A* and B* under illumination to 500 nm chopped light at 0 V applied bias (b) A magnified (on/off) photoresponse cycle for the fabricated PDs. 107

LIST OF ABBREVIATIONS

a.u.	Arbitrary unit
AFM	Atomic force microscopy
$CdCl_2$	Cadmium Chloride
CdS	Cadmium sulfide
CBD	Chemical bath deposition
CVD	Chemical vapour deposition
CHM	Composite-hydroxide-mediated
DLE	Deep-level emission
DI	Deionized water
FESEM	Field emission scanning electron microscopy
ICDD	International Centre for Diffraction Data
MA-CBD	Microwave-assisted chemical bath deposition
MSM	Metal–semiconductor–metal
NBE	Near-band-edge
PD	Photodetector
PL	Photoluminescence
QDs	Quantum dots
TE	Thermal evaporation
TU	Thiourea
2D	Two-dimensional
XRD	X-ray diffraction
EDX	Energy dispersive X-ray spectroscopy
VLS	Vapor–liquid–solid

LIST OF SYMBOLS

D	Average crystallite size
k	Boltzmann constant
Cd	Cadmium
°C	Celsius
CB	Conduction band
I	Current
I–V	Current-voltage
I_{dark}	Dark current
θ	Diffraction angle
χ	Electron affinity
q	Electron charge
E_g	Energy gap
e–h	electron–hole
A^{**}	Effective Richardson coefficient
E_F	Fermi level of metal
$E_{F,S}$	Fermi level of semiconductor
n	Ideality factor
a	Lattice constant
K	Kelvin
ϕ_M	Metal work function
M	Molar
h, k, l	Miller indices
I_{ph}	Photocurrent

η	Quantum efficiency
t_{Rec}	Recovery time
I_F/I_R	Rectifying ratio
R_{rms}	Root-mean-square
I_R	Reverse current
$I_{dark\ R}$	Reverse dark current
$I_{ph\ R}$	Reverse photocurrent
R	Responsivity
t_{Res}	Response time
ϕ_B	Schottky barrier height
ϕ_S	Semiconductor work function
S	Sensitivity
K_{sp}	Solubility product
a_o	Standard lattice constant
ε_{zz}	Strain
S	Sulfur
V_s	Sulfur vacancy
hv	The energy of the photon
β	The full width at half maximum
VB	Valence band
V	Voltage
Vs	Velocity in second
λ	Wavelength
W/mK	Watt/meter.Kelvin

SINTESIS DAN PENCIRIAN FILEM NIPIS CdS NANOHABLUR OLEH PEMENDAPAN RENDAMAN KIMIA BERBANTUKAN GELOMBANG MIKRO BAGI APLIKASI PENGESAN FOTO

ABSTRAK

Kajian ini bertujuan untuk mensintesis filem nipis kadmium sulfida berstruktur-nano (CdS) untuk peranti pengesan-foto (PD) yang cekap menggunakan kaedah mudah dan berkos rendah. Filem nipis CdS berstruktur-nano telah dihasilkan di atas substrat Si (100) oleh pemendapan rendaman kimia berbantukan gelombang mikro. Sifat-sifat filem nipis CdS yang dihasilkan telah dioptimumkan dengan mengawal parameter penghasilan seperti kepekatan molar sumber ion (Cd^{2+} and S^{2-}), tempoh penghasilan dan nisbah molar prekursor. Analisis menunjukkan bahawa filem nipis CdS nanohablur yang telah dicirikan dengan baik telah diperolehi menggunakan prekursor 0.08 M pada masa pemendapan 20 min. Morfologi permukaan filem nipis yang dihasilkan menjadi lebih padat dan seragam dan menunjukkan kekasaran yang lebih tinggi. Sifat-sifat filem nipis yang dihasilkan telah dipertambahbaik selanjutnya dengan meningkatkan nisbah molar prekursor S/Cd. Kualiti struktur filem nipis CdS yang disediakan telah dipertingkatkan dengan ketara pada nisbah molar S/Cd sebanyak 1.875. Pengukuran fotoluminesen mendedahkan pancaran yang cekap pada 510 nm, yang mana bersepadanan dengan pancaran hampir-pinggir-jalur CdS. Selain itu, ketumpatan kecacatan dikurangkan, seperti yang dicadangkan oleh intensiti rendah bagi kecacatan yang berkaitan dengan pancaran. Darjah penghabluran filem nipis yang dihasilkan juga meningkat, seperti yang ditunjukkan oleh peningkatan saiz bijian purata kristalit (D). Nilai D telah meningkat dari 36 ke 42 nm apabila nisbah molar S/Cd ditingkatkan dari 1 ke 1.875. Kesan parameter penyediaan terhadap sifat

pengesan-foto oleh filem nipis CdS yang dihasilkan juga telah dikaji. Pengesan foto (PDs) logam-semikonduktor-logam Ni-CdS-Ni telah dibangunkan dan dibuat pencirian. PD tersebut dibangunkan berdasarkan keadaan filem nipis CdS optimum (disediakan dengan menggunakan perkursor 0.08 M pada masa pemendapan 20 min). PD yang dibangunkan menunjukkan kepekaan foto dan masa tindak balas masing-masing sebanyak 1440% dan 9 ms terhadap cahaya 500 nm ketika dikenakan pincangan sonsang pada -1 V. Sifat pengesan-foto oleh PD yang dibangunkan telah bertambah baik dengan mengubah nisbah molar prekursor S/Cd. Kepekaan foto maksimum 25.28×10^{3}% dengan masa tindak balas 8 ms telah diperolehi bagi PD yang dibangunkan berasaskan filem nipis CdS berkristal-nano yang dihasilkan dengan menggunakan nisbah molar S/Cd pada 1.875 pada pincangan sonsang -1 V. PD yang dibangunkan juga mempamerkan kebocoran kecil arus gelap (1.3 μA) berbanding arus-foto yang diperolehi (330 μA) di bawah pencahayaan, yang membawa kepada peningkatan kepekaan foto peranti. PD yang difabrikasi berasaskan filem nipis CdS nanohablur yang disediakan menggunakan nisbah molar S/Cd sebanyak 1.25 dan 1.875 mempamerkan arus foto yang boleh diukur pada pincangan sonsang sifar, yang mana ianya menunjukkan bahawa peranti yang difabrikasikan adalah berkuasa sendiri. Medan terbina-dalam, yang terbentuk di dalam kawasan susutan daripada persimpangan Schottky Ni/CdS, bertindak sebagai daya penggerak untuk memisahkan pasangan elektron-lohong yang dijana-foto daripada penggabungan semula dan menjana arus-foto tanpa apa-apa pincangan luar. Pengukuran masa tindakbalas-foto mendedahkan PD yang dibangunkan boleh berfungsi sebagai peranti berkuasa sendiri dengan kepekaan foto tinggi dan masa tindak balas yang cepat masing-masing sebanyak 9.72×10^{4}% dan 10 ms terhadap cahaya berkuasa-rendah (1.20 mW/cm^2, 500 nm). Kajian ini memperkenalkan satu

pendekatan yang kos efektif dan mudah untuk membina peranti cekap dari segi kepekaan foto dan kepantasan tindak balas dengan penggunaan kuasa yang rendah mahupun kepada sifar. Peranti yang dibina berpotensi digunakan sebagai PD berkuasa rendah atau suis optik untuk aplikasi optoelektronik bersepadu secara komersial.

SYNTHESIS AND CHARACTERIZATION OF NANOCRYSTALLINE CdS THIN FILMS BY MICROWAVE-ASSISTED CHEMICAL BATH DEPOSITION FOR PHOTODETECTORS APPLICATION

ABSTRACT

This study aimed to synthesize nanostructured cadmium sulfide (CdS) thin films for efficient photodetector (PD) devices using a simple and low-cost method. Nanocrystalline CdS thin films were grown on Si(100) substrates by microwave-assisted chemical bath deposition. The properties of the grown CdS thin films were optimized by controlling the growth parameters such as the molar concentration of ion (Cd^{2+} and S^{2-}) sources, the growth duration, and the molar ratios of the precursors. Analyses revealed that a well-characterized nanocrystalline CdS thin film was obtained using 0.08 M precursors at a deposition time of 20 min. The surface morphology of the grown thin film became more compact and uniform and showed higher roughness. The properties of the grown thin films were further improved by increasing the S/Cd precursors molar ratio. The structural quality of the prepared CdS thin film was significantly enhanced at a S/Cd molar ratio of 1.875. Photoluminescence measurement revealed an efficient emission at 510 nm, which corresponds to the near-band-edge emission of CdS. Moreover, the density of defects was reduced, as suggested by the low intensity defect-related emission. The crystallinity of the grown thin films was also increased, as suggested by the increasing of the average crystallite (*D*) grain size. The *D* value was increased from 36 to 42 nm when the S/Cd molar ratio was increased from 1 to 1.875. The effect of the preparation parameters on the photodetection properties of the grown CdS thin films was investigated. Ni–CdS–Ni metal–semiconductor–metal photodetectors were fabricated and characterized. A PD was fabricated based on optimum CdS thin film

conditions (prepared using 0.08 M precursor at a deposition time of 20 min). The fabricated PD showed, respectively, a photosensitivity and response time of 1440% and 9 ms to 500 nm light at an applied reverse bias of −1 V. The photodetection properties of the fabricated PDs were improved by varying the S/Cd precursor molar ratios. A maximum photosensitivity of 25.28×10^3% with a response time of 8 ms was obtained for the fabricated PD based on a nanocrystalline CdS thin film prepared using a S/Cd molar ratio of 1.875 at a reverse bias of −1 V. The fabricated PD exhibited a small leakage (dark) current (1.3 μA) compared to the obtained photocurrent (330 μA) upon illumination, which led to an enhancement of the device photosensitivity. The fabricated PDs based on nanocrystalline CdS thin films prepared using S/Cd molar ratios of 1.25 and 1.875 exhibited a measurable photocurrent at zero applied bias, which demonstrate that the fabricated devices are self-powered PDs. The built-in field, which formed within the depletion region of the Ni/CdS Schottky junction, acts as the driving force to separate the photogenerated electron–hole pairs from recombination and generate a photocurrent without any external bias. Photoresponse measurements revealed that the fabricated PDs can function as self-powered devices with high photosensitivity and rapid response time values of 9.72×10^4% and 9 ms, respectively, to low-power (1.20 mW/cm^2, 500 nm) light. The present study introduced a cost-effective and simple approach to fabricate efficient devices in terms of photosensitivity and response speed with low power consumption, even down to zero.

CHAPTER1: INTRODUCTION

1.1 Introduction

Highly sensitive photodetectors (PDs) have received considerable attention because of their importance in several applications including the electronic industry, environmental monitoring, and space research [1, 2]. Visible light-sensing devices with high photosensitivity and selectivity, fast response and decay times, and reproducible characteristics are required for efficient photodetection applications, such as in air pollution monitoring, memory storage, optoelectronic switches, and light-wave communications [1, 3, 4]. Moreover, high-performance PDs with low power consumption are highly demanded for applications of optoelectronic integration.

It is highly desired to develop optical sensors that can power themselves without electrical power input, which could significantly enhance the adaptability of the devices and reduce the size, cost, and weight of the system. Self-powered nanodevices are expected to play a crucial role in the future of nanotechnology-based applications, mainly because of their independent, sustainable, and maintenance-free operation [5]. Therefore, metal–semiconductor–metal (MSM) PDs are generally used as visible light detectors. The formation of Schottky contact is an effective approach to achieve a large barrier height at the metal–semiconductor interface for high performance PDs [6, 7]. Consequently, a small leakage current can be obtained, which further improves the photocurrent (I_{ph}) to dark current (I_{dark}) ratio, leading to high photosensitivity.

Nanostructured semiconducting materials have received considerable attention from many disciplines because of their notable performance in electronics, optics, and photonics [8]. With reduction in size, novel electrical and optical properties are observed,

which are believed to be largely the result of surface-state and quantum-confinement effects. Group II–VI semiconductors have been researched extensively because of their outstanding optical and electrical properties and economic synthetic routes [9, 10]. Cadmium sulfide (CdS), in particular, is an important II–VI semiconductor because of its direct bandgap (2.42 eV) at room temperature and high sensitivity [11]. It is a promising material for visible light detection because it tunes emission in the visible-light range. CdS is also used in several optoelectronic applications including solar cells, thin-film electroluminescent displays, and light-emitting devices [12].

Nanostructured CdS can be prepared using different techniques including direct current electrodeposition [13], solvo/hydrothermal synthesis [14], thermal evaporation [15], and chemical bath deposition (CBD) [16]. However, CBD is considered as the simplest and a low-cost technique that produces homogeneous CdS thin films. Moreover, CBD technique assisted by microwave irradiation is a novel approach and is a rapidly developing area of research. Compared with conventional methods, microwave synthesis is more rapid and efficient; it provides rapid volumetric heating with no thermal gradients. Microwaves ensure uniform heat distribution within the synthesis vessel that plays a crucial role in improving the quality of the synthesized material [17]. The integration of microwave irradiation and CBD technique is referred to as microwave-assisted chemical bath deposition (MA-CBD).

1.2 Problem statement

CdS thin films prepared by CBD suffered from low crystallinity, which sets limits to their use in certain applications that require highly sensitive and fast response devices such as optical switches and PDs. However, most synthesis techniques require high

temperature and sophisticated instruments [14, 18-20], which raise the cost of CdS-based devices. Hence, the development of low-cost and facile synthetic strategies for high-quality nanostructured CdS thin films is very vital to the field of optoelectronics. Studies on nanocrystalline CdS thin film-based PDs are seldom reported. Moreover, CdS thin films grown on Si substrates via the CBD technique are of poor quality because of Si-induced defects during the deposition process, which leads to the deterioration of the quality of the grown thin films [21, 22]. Consequently, CdS thin film-based PDs exhibit poor performance, i.e., slow response time, especially at low illumination intensities [23].

To date, relatively little effort has been focused on low-power, or even self-powered visible light PDs that hold great promise in future nano-optoelectronic devices. However, most of the reported studies [2, 18, 24] involved complicated and costly fabrication techniques. The effect of important preparation parameters such as the molar concentration of ion sources, the deposition time, and the S/Cd molar ratio on the performance of CdS-based PDs needs to be investigated.

1.3 Scope of study

In this study, nanocrystalline CdS thin films were grown on Si substrates using simple, fast, and inexpensive preparation techniques. CBD was integrated with microwave to synthesize high-quality nanocrystalline CdS thin films on Si substrates for the fabrication of PDs. The influence of preparation parameters such as precursor molar concentration, deposition time, and the S/Cd molar ratio on the structural, morphological, and optical properties was investigated. Moreover, the effect of growth parameters on the performance of the fabricated PDSs was studied. This study seeks to cut down the cost of

the PD fabrication process. This study proposes a simple and low-cost way to fabricate low power consuming, highly photosensitive, and fast response MSM-based PDs.

1.4 Objectives of this study

The main objectives of the current study are:

1. To grow nanocrystalline CdS thin films on silicon substrates using the CBD technique aided by microwave irradiation and study the effect of growth parameters such as the molar concentration of ion sources, deposition time, and the S/Cd molar ratio on the structural, morphological, and optical properties of the grown CdS thin films.
2. To fabricate low power, highly photosensitive, and fast response CdS-based PDs using simple, fast, and a low-cost fabrication method and study the effect of thin film growth parameters on the performance of the fabricated PDs.
3. To demonstrate MSM–CdS-based highly photosensitive self-powered PDs.

1.5 Originality of this research

The originality of this study lies on the following aspects:

1. Growth of nanocrystalline CdS thin films on silicon substrates using the CBD technique aided by microwave irradiation.
2. Fabrication of highly photosensitive and fast response CdS-based PDs using simple and cost effective method.
3. Using the MA-CBD method to fabricate ultra-high photosensitive MSM-based self-powered PDs, which has not been attempted before.

1.6 Outline of the thesis

The thesis is organized into seven chapters. Chapter 1 presents a brief introduction about the current study, the research problem statement, objectives of the research, scope of work, and thesis originality. Chapter 2 presents a literature review on CdS and its important fundamental properties. The literature also included the growth of nanocrystalline CdS thin films by CBD and MA-CBD. Studies on nanostructured CdS-based PDs are also reviewed. Chapter 3 presents a theoretical background on CBD technique and MA-CBD, with thin films growth mechanism involved. The structural and optical properties of CdS thin films are presented. Theoretical concepts on metal–semiconductor contacts and the working principles of PDs are also discussed in the chapter. Chapter 4 describes the methodology and the characterization tools used to analyze the prepared material and fabricated PDs. The characterization results for the grown nanocrystalline CdS thin films are discussed in Chapter 5. Chapter 6 presents the characterization results and discussion of the fabricated CdS-based PDs. Finally, Chapter 7 presents the conclusions and the suggested future work.

CHAPTER 2: LITERATURE REVIEW

2.1 Introduction

This chapter presents a literature review on the synthesis of CdS thin films prepared by CBD technique. The preparation parameters that influence the properties of the prepared CdS thin films are discussed. Synthesis of various novel nanostructured CdS using the MA-CBD is also reviewed. Furthermore, studies on CdS-based PDs along with their characterization are reviewed also.

2.2 Literature review

2.2.1 CdS

CdS is an important group II–VI semiconductor material. It has attracted a great interest in electronic and optoelectronic devices [11]. It is a promising material for visible light detection because of its intermediate energy bandgap of (2.42 eV) and high photosensitivity [25]. The deposition of CdS was explicitly reported in 1961 by Mokrushin et al [26]. Since then, CdS has become one of the most studied compounds deposited by CBD. Nowadays, CdS is widely used as a layer for both CdTe and $CuIn(Ga)Se_2$ thin film solar cells. It also has been used in various electronic devices to passivate surfaces [27, 28]. CdS has good thermal stability, light fastness, chemical resistance and high opacity, make it as a potential material for optoelectronic applications. Table 2.1 summarizes important properties of CdS.

Table 2.1: Electrical, thermal, mechanichal and optical properties for CdS

Electrical properties	
Dielectric Constant	8.9
Electron Mobility	350 cm^2/Vs
Hole Mobility	40 cm^2/Vs
Band Gap	2.42 eV
Thermal Properties	
Thermal Expansion Coefficient	H= 6.26×10^{-6}/K C= 3.5×10^{-6}/K
Thermal Conductivity	40.1 W/mK
Mechanical Properties	
Melting Point	1750°C
Boiling Point	980°C
Density	4.826 g/cm^3
Optical Properties	
Refractive Index	2.529

2.2.2 Nanocrystalline CdS thin films prepared by CBD

Several studies have been reported on the growth of nanocrystalline CdS thin films using the CBD technique. Nanostructured CdS exhibits novel structural, optical, electronic, and photoconducting properties compared to its bulk counterparts [29, 30]. Accordingly, the synthesis of nanostructured CdS thin films has attracted tremendous

attention because of their potential in optoelectronic devices, such as thin-film electroluminescent displays [31], optical wave guides [32], and in the manufacture of highly efficient solar cells [33, 34]. CdS nanostructures can be synthesized using several techniques, such as screen printing [35], molecular beam epitaxy [36], chemical vapor deposition [37], thermal evaporation [38], pulsed laser deposition [39], and CBD [16]. Compared to other techniques, CBD is attracting considerable attention in the synthesis of nanostructured CdS thin films. It is a relatively inexpensive, simple, and convenient method for large area deposition. Furthermore, using the CBD method, a large number of different substrates in various shapes and sizes can be coated in a single run [40].

The properties of the produced thin films are significantly affected by the preparation parameters. Khallaf et al. [41] prepared CdS thin films on glass substrates using the CBD technique with different cadmium ion (Cd^{+}) sources. The effect of different Cd^{2+} sources on the properties of the prepared CdS thin films was comprehensively studied and reported. Liu et al. [42] studied the influence of ammonia concentration on stoichiometry, surface morphology, and optical properties of CBD-CdS thin films on glass substrates. The results revealed that the properties of the prepared films depended significantly on the initial concentration of ammonia in the deposition bath. Uniform and compact CdS thin films were obtained when the ammonia concentration was in the range 0.8–2.0 M. The films deposited with an ammonia concentration of 1.0 M showed the highest degree of crystallinity and closest to a Cd/S stoichiometry of ~1.

Kariper et al. [43] investigated the influence of the pH of the solution on the physical properties of CdS thin films. The study showed that structural, electrical, and optical properties of the deposited films are sensitive to the pH value of the chemical

bath. It has been found that a pH value of 10 is suitable for producing low resistivity CdS films by the CBD technique, feasible for technological purposes, especially for solar cells.

The effects of molar concentration of precursors on the properties of CBD-CdS thin films have been studied by several authors [44-52]. Sandoval-Paz and Ramírez-Bon [51] studied the optical and structural properties of CBD-CdS thin films prepared on polyethylene naphthalate substrates as a function of the cadmium content in the precursor solution. Increasing Cd concentration in the reaction solution yields thicker CdS films with smaller grain size and higher energy bandgap. Ximello-Quiebras et al. [46] studied the effect of thiourea (TU) concentration on the properties of CdS thin films grown on SnO_2:F conducting glass by the CBD technique. It has been found that the growth rate for CdS thin films is faster when the quantity of TU is much greater than the cadmium chloride concentration in the solution. In addition, the bandgap value for the prepared thin films increased at higher S/Cd ratio.

Gopinathan et al. [50] prepared CdS thin films on glass substrates by CBD using different S/Cd molar ratios. Thin films prepared using equal molecular ratios of Cd and S were amorphous in nature. The crystallinity of the prepared films increased with increasing S/Cd ratio in the precursor solutions. Sasikala et al. [49] studied the effect of Cd ion concentration in the solution, revealing that changing Cd concentration significantly affects the optical and electrical properties of the grown CdS thin films because of the change in their crystallinity. Increasing the Cd concentration drives the crystallization of CdS thin films from cubic to the hexagonal phase, which is more suitable for solar cells fabrication. Mendoza-Pe´rez et al. [52] studied the effects of TU molar concentration on CdS thin films grown by CBD for CdS/CdTe-based solar cells. It

was found that the performance of the solar cells increased with increasing the S/Cd ratio in the CBD solution. A better performing solar cell was obtained for CdS thin films grown at a S/Cd molar ratio of 5.

Furthermore, studies have been reported on the effect of deposition time on the properties of CBD-CdS thin films. Moualkia et al. [53] studied the effect of deposition time on CBD-CdS thin films in an attempt to optimize their optoelectronic properties. The conductivity of the prepared thin films was examined as a function of deposition time. CdS thin films prepared at low deposition times present a relatively high dark conductivity. At low deposition time, the concentration of the sulfur vacancy (V_s) that contributes to the dark current is large, since these defects behave as donor defects. However, the photoconductivity of the prepared thin films was found to increase with increasing deposition time. Such improvement in photoconductivity is associated with the improvement of the crystalline structure of the grown thin films as suggested by the increase in the grain size with increasing deposition time.

Lincot and Ortega-Borges [54] reported an in-situ analysis of the CdS deposition process by CBD. They found that the growth of the CdS films occurs in two successive steps, the formation of a dense compact inner layer followed by the formation of a porous external layer. A compact CdS layer is formed at the earlier growth stages by the ion-by-ion process, whereas the external porous CdS layer is formed at larger deposition times by the cluster-by-cluster process.

Sandoval and Ramírez [55] studied the early growth stages of CdS thin films during chemical deposition. A series of deposition times between 6 and 35 min was chosen to determine the precise time at which the growth switches from ion-by-ion to

cluster-by-cluster mechanism. It has been found that the ion-by-ion growth mechanism occurs at deposition times of up to 15–18 min where homogeneous, continuous, and crystalline CdS layers covering the entire substrate area were obtained. With longer deposition times between 15 and 18 min, cluster-by-cluster growth begins and a porous layer is formed on top of the compact layer. Using lower reagent concentrations in the reaction solution promoted only the ion-by-ion growth in all the ranges of the studied deposition times.

2.2.3 Nanostructured CdS prepared by MA-CBD

Microwave irradiation induces the interaction of the dipole moment of polar molecules with alternating electronic and magnetic fields, causing molecular-level heating, which leads to homogeneous and quick thermal reactions [56, 57]. In fact, microwave irradiation in water can produce high energy values that are needed for the creation of nanoparticles, where the growth process can be performed in a short time [58]. Hence, microwave heating is considered as an efficient and promising method for the rapid preparation of inorganic nanostructures in solvents [59]. Several studies have recently been reported on the synthesis of various and novel nanostructured CdS by MA-CBD approach.

Nirmal et al. [60] conducted a comparison study for CdS nanocrystals prepared by microwave irradiation and conventional heating process. Highly monodispersed CdS nanoparticles of ~5 nm were obtained in a short time using the microwave irradiation process. Zhu et al. [61] repoetred the synthesis of CdS nanoribbons by microwave irradiation. CdS nanoribbons of about 4 nm in diameter have been prepared in a rapid synthesis route. Microwave heating afforded the formation of uniform nanosized particles With microwave irradiation of reactants in polar solvents, temperature and concentration

gradients can be avoided, providing a uniform environment for the nucleation. Results demonstrate the higher energy produced by microwave to promote the reactionsto form CdS nanoribbons.

Mahdi et al. [62] studied the effect of the molar concentration of reagents on the properties of nanocrystalline CdS thin films prepared via MA-CBD. It has been found that varying the molar concentration of Cd^{+2} sources significantly affected the physical properties of the grown CdS thin films. Li et al. [63] prepared highly photocatalytic, active CdS/TiO_2 nanocomposites by combining CBD and microwave-assisted hydrothermal synthesis. All the as prepared CdS/TiO2 nanocomposites exhibited anatase TiO_2 and hexagonal CdS phases. Besides, the morphologies of CdS/TiO_2 nanocomposites were clearly affected with increasing the deposition time. The initial popcorn-like structure changed to wedge-like structure.

Li et al. [64] first demonstrated the synthesis of CdS/kaolinite nanocomposites by assembling CdS nanoparticles on the surface of kaolinite rods using the microwave irradiation process in aqueous solution. The enhanced properties of CdS/kaolinite compared to pure CdS nanoparticles indicated its potential applications in the optoelectronic fields. Bao-yun et al. [65] synthesized hierarchical, hollow, spherical CdS nanostructures via a hydrothermal process in a shorter time and lower temperature than common hydrothermal methods with the aid of microwave irradiation. SEM and TEM images show that the hierarchical hollow spherical CdS nanostructures with a diameter range of 400-600 nm are self-assembled by nanoparticles of 30 nm. The XRD patterns and EDS spectrum demonstrate that the products are well crystallized with high purity.

Ebadi et al. [58] investigated the effect of microwave time and power and precursor concentration on the size and morphology synthesis of CdS/Bi_2S_3 nanocomposite product from aqueous solutions. It was found that the optimum condition for the production of separated nanoparticles was done in 9 min and 750 W microwave irradiation. Zhu et al. [66] deposited CdS quantum dots (QDs) on the surface of TiO_2 films for QD-sensitized solar cells using MA-CBD. The results revealed that solar cells based on MA-CBD-CdS QDs showed an improved short-circuit current density and power conversion efficiency compared to those employing the conventional sequential CBD method. Using the MA-CBD method, the nucleation and growth of CdS QDs was achieved in an extremely short period of time, which is extraordinarily beneficial for reducing the concentration of surface defects of QDs.

Murugan et al. [67] presented a novel process of microwave–solvothermal technique for synthesizing nanocrystalline CdS particles. The effect of different parameters such as time, temperature and molar ratio of Cd^{2+} to thiourea on the phase formation of nanocrystalline cadmium sulfide was investigated. It was found that the higher molar ratio of TU to $CdSO_4$ is favorable for producing the hexagonal CdS phase and smaller particles. Ni et al. [68] successfully prepared an array of CdS nanotubes in a porous anodic alumina membrane under the assistance of microwave irradiation, using $CdCl_2$ and thiourea. TEM and SEM analyses clearly demonstrate the formation of of CdS nanotubes with a mean diameter of 200 nm.

Tai et al. [69] synthesized complex three-dimensional flower-like CdS nanostructures using sonochemistry-assisted microwave synthesis. Different structures of hexagonal nanopyramids and nanoplates single-crystalline CdS were obtained depending on different sulfur sources. The reaction temperature, duration and different sulfur

sources have significant effect on the morphology of the synthesized CdS nanostructures. Optical characterization of the complex three-dimensional flower-like CdS nanostructures showed a large blue-shift up to 100 nm in comparing with simple low-dimensional CdS nanostructures. The induced shift in optical properties may have potential applications in optoelectronics devices, catalysis, and solar cells.

2.2.4 Nanostructured CdS-based PDs

Visible light detection plays a crucial role in several applications, including optical switches or PDs, environmental monitoring, and space research [1]. Furthermore, in many of these applications, a high processing speed of the device is critical. Therefore, there is a strong demand to develop reliable, rapid response, and highly sensitive devices. CdS is a promising material for PDs that can sense visible radiation of the electromagnetic spectrum because of its proper bandgap (2.42 eV). Numerous studies have been devoted on the fabrication of CdS-based PDs using different approaches.

Oladeji et al. [23] studied the photoconductivity of CdS thin films deposited by single, continuous, and multiple dip chemical processes. They found that the peak photocurrent of the grown CdS thin films depends on the film thickness. However, thin films prepared using the single dip process showed a faster response time than those prepared using the multi- and continuous dip process. The slower response time is due to the high density of trap states for thin films prepared using the multi-dip process.

Abdulrazaq and Saleem [4] fabricated near-IR CdS/Si heterojunction-based PDs by a chemical spray pyrolysis technique at different preparation substrate temperatures. It was found that the PD properties were affected by the substrate temperatures. The rise time of the photocurrent was faster at a CdS preparation temperature of 400 °C.

Amos et al. [70] fabricated CdS PD arrays on transparent flexible polyethylene terephthalate sheets from an aqueous solution of $CdCl_2$ and TU. The detectivity and the time-dependent photoresponse of the fabricated PDs were further improved by increasing the TU molar concentration upon illumination with 514 nm laser at different power densities. Sulfur vacancies that contribute to the carrier concentration are reduced with the introduction of more sulfur precursors during growth that led to a decrease in the dark current. This suggests an enhancement of the PDs performance.

Salwan et al. [71] studied the optoelectronic properties of n-CdS/p-Si and n-CdS:In/p-Si heterojunction PDs prepared by thermal evaporation. They found that the spectral response of the PDs was highly improved after doping indium into CdS films at optimum conditions. The highest value of the response was 0.46 AW^{-1} at 800 nm for doped CdS prepared at an indium diffusion temperature of 300 °C. The indium-doped CdS film led to an improved junction interface quality and consequently diode characteristics.

Yang et al. [2] fabricated single-nanowire-based CdS PDs using microbial fuel cell (MFC). The device was sensitive to multicolor light ranging from red to UV light. Furthermore, the device exhibited response and decay times of 30 and 40 ms, respectively, to solar light. Li et al. [72] studied the optoelectronic characteristics of single-crystalline CdS nanobelt-based PD fabricated by thermal evaporation with Au as a catalyst. The rise time was 91 ms, and decay time was 864 ms on illumination with green laser. Chen et al. [73] found that the rise and decay times of single crystal CdS nanoribbons to 515 nm laser fabricated by thermal evaporation were 200 and 500 ms, respectively. Xi et al. [74] reported a rise time of 1.0 s and a decay time of 0.2 s for a single CdS nanowire-based PD fabricated by the composite hydrothermal method (CHM)

when illuminated by simulated sunlight. Wei et al. [1] studied the effect of the contact type on the detection ability of the CdS nanowire-based PD. They found that the sensitivity of the Schottky contact device to white light was 58 times higher than that of the corresponding ohmic contact. Mahdi et al. [75] studied the photoelectric properties of a single-crystalline microrod CdS-based PD fabricated via a thermal evaporation technique. The device showed a fast response time to 460 nm light at different applied biases with high sensitivity. Moreover, Gao et al. [76] reported a response time of 1–3 s for single-crystalline CdS nanobelt-based photoconductors prepared by the thermal evaporation of CdS powders.

After an extensive literature review, it was concluded that no study has been reported on the fabrication of PDs based on nanocrystalline CdS thin films by employing the microwave irradiation approach. This is the main motivation behind the current studies investigating the effects of the MA-CBD method on the fabrication and characterization of efficient CdS-based optical sensors. Furthermore, low power, rapid response CdS-based PDs are seldom reported. Table 2.2 summarized the photoresponse properties of CdS-based PDs fabricated using different approaches.

Table 2.2: Photoresponse properties of CdS-based PDs fabricated using different fabrication methods.

Fabrication method	Structure	Wavelength (nm)	Intensity (mW/cm^2)	Applied bias (V)	Rise time (ms)	Fall time (ms)	Ref.
CBD	Thin film-based	White	50	10	150	300	[23]
Spray pyrolysis	Thin film-based	1000	---	---	$60x10^{-5}$	---	[4]
Chemical solution	Thin film- based	514	17.80	60			[70]
Thermal resistive	Thin film-based	800	100	3.00	$200x10^{-4}$		[71]
MFC	Nanowire-based	Solar light	3.0	0.0	30	40	[2]
Thermal evaporation	Nanobelt-based	510	30.0	0.0	91	864	[72]
Thermal evaporation	Nanoribbon-based	515	400.00	3.0	200	500	[73]
CHM	Nanowires-based	White	100.00	10.00	1000	200	[74]
PVD	Nanowires-based	White	---	-8.00	572	320	[1]
Thermal evaporation	Micro-rod-based	460	1.20	3.00	32	38	[75]
Thermal evaporation	Nanobelt-based	White	---	---	1000	1000	[76]

CHAPTER 3: THEORETICAL BACKGROUND

3.1 Introduction

This chapter presents a theoretical background on CBD and MA-CBD along with thin films growth mechanism involved. The chapter also comprises theoretical concepts of the structural and optical properties of CdS. Metal semiconductor contact theory and theoretical concept of PDs with their operational parameters are discussed.

3.2 CBD technique

Considering the current interest in nanostructured materials because of their potential application prospects, CBD has been extensively utilized for the synthesis of nanostructured semiconductors because of the low cost synthesis route and high production scale. CBD is the most common solution process used to deposit CdS thin films [77]. Chemical deposition refers to the deposition of films on a solid substrate from a reaction occurring in an aqueous solution.

CBD is the experimentally simplest method in chemistry and material syntheses as it does not require sophisticated instrumentation and other expensive equipment. The chemicals used in the synthesis process are commonly available and cheap. Moreover, high temperature is not required; the reaction between the dissolved precursors occurs generally in aqueous solution at low temperature (30 °C to 80 °C) [78]. Various substrates such as insulators, semiconductors, or metals can be used since these are low temperature processes that prevent oxidation and corrosion of the substrate. CBD is not a new technique; it originated more than a century ago.

As early as 1835, Liebig [79] reported the deposition of thin film silver mirror for the first time using this technique. In 1884, Emerson-Reynolds [80] reported the deposition of PbS films from aqueous solutions of TU and alkaline lead tartrate. CBD was then essentially limited to PbS and PbSe for a long time until 1961 when CdS thin films were explicitly reported by Mokrushin et al. [26] The range of materials deposited by CBD was gradually expanded, particularly in the 1980s, to include a large number of semiconductors of metal chalcogenides due to their potential in optoelectronic applications [79].

Chemical deposition received a major impetus after CdS was used as a window layer for CdS/CdTe and CdS/$CuInSe_2$ thin film-based solar cells [81, 82]. It has been found that CdTe and $CuInSe_2$-based solar cells showed superior photovoltaic performance with the CBD-CdS thin films compared to evaporated CdS [83, 84]. Therefore, the CBD method allows for the manufacture of relatively low cost devices, especially light detectors and light energy conversion cells [85]. However, few studies reported on the growth of CdS thin films on Si substrates by the CBD technique [21, 22, 86].

CdS thin films grown on Si substrates by the CBD technique are of low crystallinity and poor quality, which limit their use in certain applications [21]. The microwave heating method is unique in providing a scaled-up deposition process that would potentially improve the synthesis of nanomaterials [60]. It can be used in conjunction with chemical deposition to improve the synthesis process of conventional heating methods and to reduce the required time of synthesis. Microwave irradiation ensures homogenous distribution of temperature within the synthesis vessel (homogeneous volumetric heating) with no thermal gradients. This process is more efficient than that achieved by a conventional method; it can solve the problems of

temperature gradients and provide uniform growth media that play a crucial role in improving the quality of the synthesized material [17]. Hence, the integration of microwave irradiation and CBD technique (referred to as MA-CBD) was utilized to synthesize high-quality nanocrystalline CdS thin films on Si for the fabrication of efficient and cost-effective PDs.

3.2.1 Mechanisms of the CBD technique

It is necessary to understand the basic terminologies of the CBD deposition process in order to better understand the growth mechanisms involved. An important concept is the solubility product (K_{sp}). It gives the solubility of a sparingly soluble ionic salt [79]. When a sparingly soluble ionic salt, let us say (AB), is dissolved in water, a solution containing A^+ and B^- ions in contact with the undissolved solid AB is obtained, as can be shown by Eq. 3.1 [78]:

$$AB(S) \leftrightarrow A^+ + B^- \tag{3.1}$$

At saturation, equilibrium is reached between the two; the solubility product is equal to the ionic product of cations and anions and thus

$$AB(S) = A^+ + B^- \tag{3.2}$$

By applying the law of mass action, Eq. 2.2 can be written as follows:

$$K = \frac{C_A^+ + C_B^-}{C_{AB}} \tag{3.3}$$

where C_A^+, C_B^- and C_{AB} are the respective concentrations of A^+, B^-, and AB in the solution. Since the concentration of pure solid AB is a constant number, thus $C_{AB} =$ a constant $= K'$

Eq. 3.3 can be written as follows:

$$K = \frac{C_A^+ + C_B^-}{K'} \quad \text{or} \quad KK' = C_A^+ + C_B^- \tag{3.4}$$

The KK' product is also constant and can be denoted by K_{SP}, therefore Eq. 2.4 becomes

$$K_{SP} = C_A^+ + C_B^- \tag{3.5}$$

K_{SP} is known as the solubility product constant. When the ionic product exceeds the solubility product, the solution is in super saturation, and growth occurs [78]. Eq. 2.5 indicates that the molar concentration of the ion source materials is an important parameter for thin film growth. For CdS, the K_{sp} is ~10^{-28} [79]. When the ionic product of Cd^+ and S^- exceeds the solubility product of CdS, the growth of thin films will begin. The growth of film occurs with two possible mechanisms, either through the ion-by-ion mechanism by the condensation of Cd^{2+} and S^{2-} ions on the substrates or by the cluster-by-cluster mechanism by adsorption of colloidal CdS from the solution.

The ion-by-ion mechanism results in thin, hard, and highly adherent films that show specular reflection. In contrast, thin films obtained by the cluster mechanism are thick, powdery, and poorly adherent to the substrates. However, CdS thin film growth is based on the slow release of Cd^+ ions and S^- ions in an alkaline solution. A Cd salt (such as $CdCl_2$) in solution can be converted to CdS by adding sulfide ions (TU). The deposition of high quality CdS thin films is based on the control of CdS precipitation in

the bath. Precipitation control can be achieved by controlling the concentration of free cadmium metal ions [Cd^{+}]. To slow the release of Cd ions, ammonia is generally added as an efficient complexing agent for Cd ions to control the concentration of cadmium metal ions. Cd salt complexes with ammonia to form the dominant tetra-amino-cadmium complex ion $Cd(NH_3)_4^{2+}$, which results in the release of small concentrations of Cd^{2+} ions upon dissociation, as described by Eq. 3.6 [42]:

$$Cd(NH_3)_4^{2+} \rightarrow Cd^{2+} + 4NH_3 \quad (3.6)$$

Sulfide ions are released by the hydrolysis of TU, as described by Eq. 3.7:

$$(NH_2)_2CS + 2OH^- \rightarrow S^{2-} + CN_2H_2 + 2H_20 \quad (3.7)$$

The $Cd(NH_3)_4^{2+}$ complexes are adsorbed on the substrates. Thereafter, heterogeneous nucleation and thin film growth occurs by the ionic exchange reaction with S^{-}, as described in Eq. 3.8 [43]:

$$Cd(NH_3)_4^{2+} + S^{2-} + CN_2H_2 + 2H_20 \rightarrow CdS + CH_2N_2 + 2H_2O + 4NH_3 \quad (3.8)$$

In this process, CdS thin films are formed on the substrates directly by the ion-by-ion mechanism. When the complex cations are insufficient, colloidal $Cd(OH)_2$ is formed and reacts with S^{2-} ions, which diminished the free Cd^{2+}. Thin films are formed by the adsorption of CdS colloids or clusters formed in the solution. In this case, adding more ammonia is required to control the OH^{-} concentration and form the tetra-amino-cadmium complex. The growth of thin films in this process is referred to as the cluster–cluster mechanism. This process yields CdS films that adhere poorly to the substrates and are of inferior quality. Important parameters such as pH, molar concentration of reactants, and

the temperature are considered to avoid cluster precipitation during the reaction and optimize the growth process. Figure 3.1 illustrates the growth of CdS thin films according to the involved mechanisms.

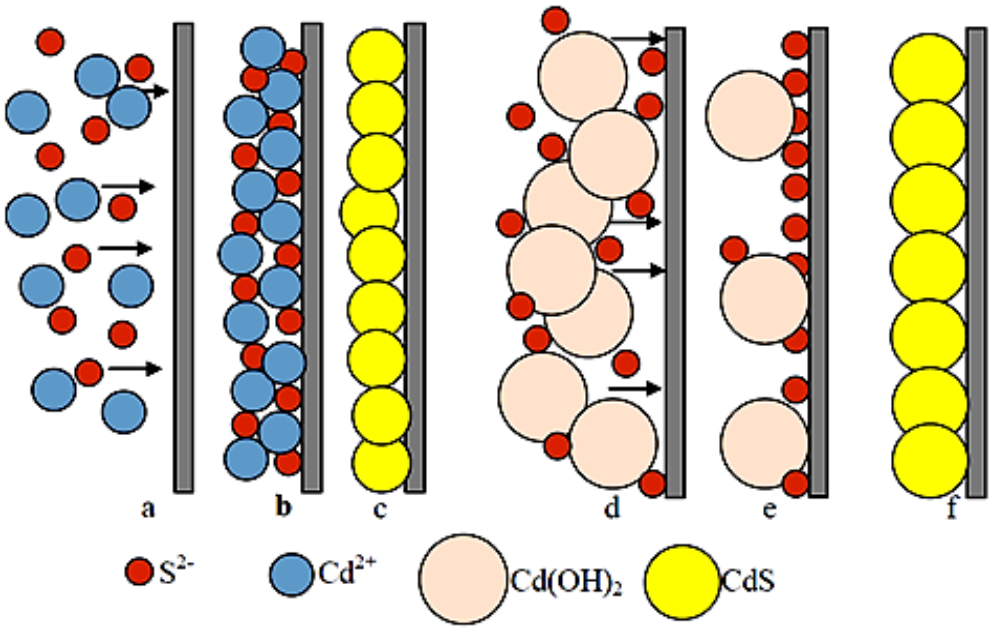

Figure 3.1: Schematic of CBD-CdS thin film via (a, b, and c) ion-by-ion mechanism and (d, e, and f) cluster mechanism. Adopted from [53].

3.2.1 MA-CBD

Microwave heating in chemical reactions is a new approach. It was initially used in 1986 for the synthesis of different organic materials [87]. Since then, the microwave heating method has received considerable attention in chemical and material syntheses. Microwave-assisted synthesis is characterized by the significant reduction of reaction times because of the solvent superheating effect, which is not achieved with traditional heating sources. Microwave ensures rapid volumetric heating with no thermal gradients [88, 89]. Using microwave, heat is generated from inside the material by the direct interaction with the microwave radiation, unlike in conventional heating methods in

which heat is transferred through conduction and convection creating thermal gradients (Figure 3.2).

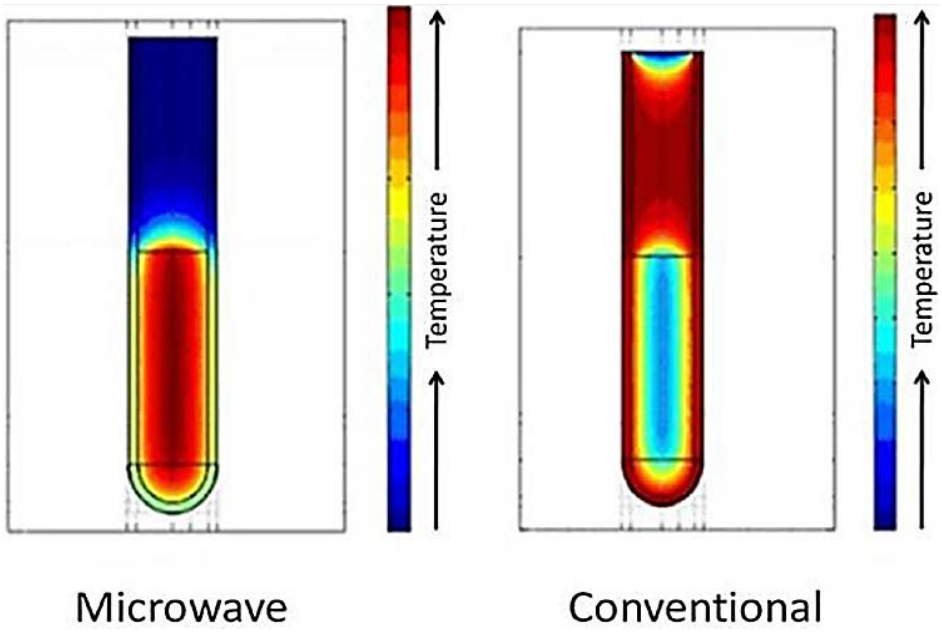

Figure 3.2: Uniform distribution of heat inside the reaction vessel using microwave compared with temperature gradients occurred by the conventional heating method [65].

Microwave irradiation induces the interaction of the dipole moment of polar molecules with alternating electronic and magnetic fields, causing molecular-level heating, which leads to homogeneous and quick thermal reactions [56, 57]. Microwaves produced by magnetrons are electromagnetic waves containing electric and magnetic field components with a frequency range between 0.3 and 300 GHz. Frequency windows that are centered at 0.9 and 2.45 GHz are allowed for microwave heating purposes [90]. Microwave heating effects are based on the impact of microwaves with polar materials/solvents. The heating effects can be understood in terms of electric dipoles in a material that follow the alternating electric component of the electromagnetic microwave.